

# Phage Display-Mediated Immuno-Multiplex Quantitative PCR for the Simultaneous Quantification of IFN- $\gamma$ and IL-6

Zhou Hu,<sup>#</sup> Shen Li,<sup>#</sup> Hanyi Chen,<sup>#</sup> Zhuoying Yu, Wenjuan Wang, Xiaotian Zhang, Mengyuan Yu, and Jianxun Wang\*



Cite This: *ACS Omega* 2025, 10, 2260–2268



Read Online

ACCESS |



Metrics & More

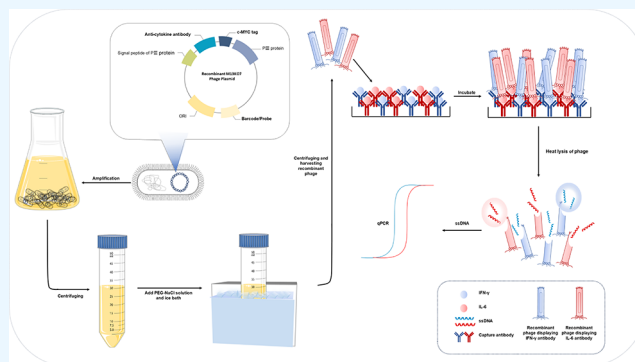


Article Recommendations



Supporting Information

**ABSTRACT:** In phage display technology, exogenous DNA is inserted into the phage genome, which generates a fusion protein with the phage coat protein, facilitates expression and promotes biological activity. This approach is primarily used to screen antibody libraries owing to its high library capacity and fast technical cycle; additionally, various types of genetically altered antibodies can be easily produced. In this study, we fused the pIII structural protein of the M13K07 phage with a scFv created by connecting the VH and VL domains of an anti-IFN- $\gamma$  antibody. Western blotting and phage immunoprecipitation demonstrated that the recombinant phage can specifically bind to IFN- $\gamma$ . After determining the amplification efficiency of the recombinant phage, we developed a PD–IPCR-based test for the cytokine IFN- $\gamma$ . The method's linear range, detection limit, blank spiking recoveries, and stability were ascertained via a standard curve; the ability of PD–IPCR to target IFN- $\gamma$  was compared with that of traditional ELISA, and the results of the two assays were consistent. Once the feasibility of using PD–IPCR to target individual cytokines was verified, we established a dual PD–IPCR quantitative assay based on a Taqman probe for IFN- $\gamma$  and IL-6 in the same system, demonstrating the feasibility of the phage display technology constructed herein for multiple cytokine detection.



## 1. INTRODUCTION

Cytokines are small, soluble peptide proteins that are biologically active and are secreted by both immune and some nonimmune cells. As signaling molecules, cytokines play critical roles in the onset and progression of various diseases and biological processes.<sup>1,2</sup> Rather than functioning as individual entities, cytokines work together to regulate physiological responses, creating a complex cytokine regulation network.<sup>3,4</sup> However, abnormalities in cytokine secretion often lead to the development of diseases, such as cytokine storms.<sup>5,6</sup> The ability to accurately quantify cytokines is crucial for understanding physiological and pathological processes and aiding in diagnosis and treatment in clinical and research settings.<sup>7–9</sup> The enzyme-linked immunosorbent assay (ELISA) is the most common method used to quantify cytokines;<sup>10</sup> this method is reliable but cannot be applied in multiplexed assays.<sup>11</sup> Considering the network nature of cytokines, multiple cytokine assays, such as cytometric bead array (CBA),<sup>12</sup> Luminex,<sup>13</sup> and Meso Scale Discovery (MSD)<sup>14</sup> assays, have flourished in recent years. However, these methods require expensive laboratory instruments and skilled technicians, and their kits are expensive.

Phage display-mediated immuno-PCR (PD–IPCR)<sup>15</sup> combines the cost-effectiveness and high sensitivity of phage

display technology<sup>16</sup> and immuno-PCR,<sup>17</sup> offering a wide-range of applications and development prospects. This method has been widely used to detect crop toxins and disease markers quantitatively,<sup>18–21</sup> but little research on cytokine detection has been performed.<sup>22</sup>

On the basis of the PD–IPCR technique in conjunction with nanobodies, we created a novel method called phage display-mediated immuno-multiplex quantitative PCR (PD–IMPCR) for the simultaneous quantification of IFN- $\gamma$  and IL-6 in the same system. PD–IMPCR uses different probes to label different recombinant phages displaying anticytokine antibodies that can bind to the corresponding cytokine and be detected by qPCR. We demonstrate the feasibility and application of this method using IFN- $\gamma$  and IL-6 as assay targets, and the results are detailed below.

**Received:** October 22, 2024

**Revised:** December 27, 2024

**Accepted:** December 30, 2024

**Published:** January 10, 2025



Table 1. Primers used in this Study

Number	Sequence (5'to3')	T <sub>m</sub> (°C)	Purpose
P1	GCGGCCGAGAACAAAACTCATCTCAGAAGAGGATCTG	69	Preparation of anti-IL-6 and IFN- $\gamma$ recombinant phages
P2	CAGATCCTCTTCTGAGATGAGTTTTTTGTTCTGCGGCCGC	70	
P3	CTTCCCTGTAAAGTATCTTCTCCTGGCATCTTCCAGGAAATC	65	SYBR Green
P4	GGAAGATACTTAAACAGGGAAGTGAGAGGGCCGCGGCAAAGC	71	
P5	TTCAGCGGAGTGAGAATAGAAAGGAACAATAAAGGAATTGC	72	
P6	GTTGTTCTTTCTATTCTCACTCCGCTGAAGAAGTGCAGTTAGTTGAGAG	53	
P7	CTTCTGAGATGAGTTTTTTGTTCTGCGGCCGCTTAATTTCCACTTTGGTGC	52	
P8	CCTTTAGTTGTTCTTTCTATTCTCACTCCGCTGAACATAGTCAGGTTTCAGCTGGTGCAG	61	
P9	GATCCTCTTCTGAGATGAGTTTTTTGTTCTGCGGCCGCACGTTCACTTCAACTTTGG	54	
P10	ACTGCGGCGAGCGGAAAT	54	
P11	GCCACCACTGATTTGAGCG	52	
P12	CTATTCTCACTCCGCTGAAACTGTTGAAAGTTGTTTAGC	53	
P13	CTTCCCTGTAAAGTATCTTCCGAACGACCGAGCGTAGCGA	63	
P14	TAACAACCTGGACCGACCGGGCTTACGAACGGGGCGGAG	72	Preparation of the recombinant phage for dual assays
P15	CGGTCCGTCAGTTGTTAATTTCCGCTCGCCGCAGTCG	72	
P16	TCTGGCTCTGCGTGTGTGCTCCCGGCTTACGAACGGGGCGGAG	69	Taqman probe-based qPCR
P17	GGGAGCACAGCACGACGAGCCAGAATTTCCGCTCGCCGCAGTCG	65	
P18	ACTGCGGCGAGCGGAAAT	63	
P19	GCCACCACTGATTTGAGCG	59	
P20	FAM-AACAACCTGGACCGACCG-BHQ1	57	
P21	CYS-CTGGCTCTGCGTGTGTGCTC-BHQ2	66	

## 2. MATERIALS AND METHODS

**2.1. Strain and Plasmid.** Beijing Tiangen Biochemical Technology Co., Ltd., provided *E. coli* DH5 $\alpha$ , and we created the M13KO7 phage genome plasmid M13KO7-MYC modified with a c-MYC tag in our laboratory. We used IFN- $\gamma$  for detection. We subsequently retrieved IFN-HuZAF, the monoclonal antibody sequence corresponding to the antibody drug fontolizumab for IFN- $\gamma$ , and ALD-518, the monoclonal antibody sequence corresponding to the antibody drug clazakizumab for IL-6, from the IMGT database. Next, we spliced the heavy- and light-chain variable regions of the antibodies into the scFv sequence, which was connected in the middle by (GGGS)<sub>3</sub>. The scFv sequence was synthesized by Suzhou Jinwei Zhi Biotech Co., Ltd., and cloned and inserted into the puc57 vector. PCR was performed with high-fidelity heat-stabilized PCR enzymes (Takara, Tokyo, Japan), and 1.25 U of enzyme, 50 ng of template, 200  $\mu$ M dNTPs, 5  $\mu$ L of 10 $\times$  buffer, and 0.5  $\mu$ M each of forward and reverse primers were added to the PCR tube to a final volume of 50  $\mu$ L. The step program for PCR was 95  $^{\circ}$ C for 3 min, 35 cycles of 95  $^{\circ}$ C for 30 s, the annealing temperature was set according to T<sub>m</sub> in Table 1 for 30 s, and the extension time at 72  $^{\circ}$ C was 1 min/kb (template provided in the Supporting Information). Following primer PCR of the pertinent template pieces, homologous recombination via the DNA Assembly Mix Plus Seamless Cloning Kit (Lablead, Beijing, China) produced the recombinant vectors used in this investigation; 5  $\mu$ L of DNA Assembly Mix, 50 ng of linearized vector, and 100 ng of insert fragment were added to the PCR tube to a final volume of 10  $\mu$ L, and the step program for recombination was 50  $^{\circ}$ C for 30 min. The primer pairs P1/P3, P4/P5, and P12/P13 were used to extract fragments 1, 2, and 5 from the M13KO7-MYC plasmid, whereas P6/P7 and P8/P9 were used to amplify segments 3 and 4 from the puc57 plasmid. Amplification from the puc57 plasmid produced pieces 3 and 4, which were then fused with fragments 1/2/3 to create the recombinant vector M13KO7-ALD-518, with fragments 1/2/4 used to create the

recombinant vector M13KO7-IFN-HuZAF and fragments 1/5 used to create the recombinant vector M13KO7 for blocking. The recombinant vector M13KO7-ALD-518 genomic plasmid was used as a template, primer pairs P1/P15 and P2/P14 were amplified to generate fragments 6 and 7, and the fusion of fragments 6 and 7 formed the recombinant vector M13KO7-ALD-518 probe. Amplification yielded fragments 8 and 9, and fusion of fragments 8 and 9 yielded the recombinant M13KO7-IFN-HuZAF probe vector (Table 1). Transformation of the above recombinant vectors into the DH5 $\alpha$  *E. coli* strain produced recombinant phages.

**2.2. Preparation of Phages.** DH5 $\alpha$  competent cells transformed with the recombinant phage plasmid were inoculated into 2 $\times$  YT culture media supplemented with 50  $\mu$ g/mL kanamycin and then incubated overnight at 37  $^{\circ}$ C with shaking at 250 rpm. The mixture was subsequently centrifuged twice at 6800 g/min for 15 min at 4  $^{\circ}$ C, ensuring that no obvious precipitate remained in the supernatant, which contained phage particles. The supernatant was transferred to a new tube, 2 mL of PEG-NaCl (PEG-8000 20% w/v; NaCl 2.5 M) solution was added, and the mixture was mixed thoroughly by inversion to precipitate the recombinant phage particles. After incubation on ice for 1 h, the mixture was centrifuged at 11000 g/min and 4  $^{\circ}$ C for 30 min. The supernatant was carefully discarded to prevent phage loss, and the cells were resuspended in 1 mL of PBS. The phage dissolved in PBS was filtered through a 0.22  $\mu$ M filter and stored at 4  $^{\circ}$ C.

**2.3. SYBR Green-Based PD-IMPCR.** To initially validate the feasibility of this method, we used SYBR Green-based PD-IMPCR to detect a single cytokine. IFN- $\gamma$  is shown as an example in this paper. Then, 50  $\mu$ L of a capture antibody (1:250 dilution; Sino Biological, Beijing, China; Cat. # 11725-R238) diluted in coating solution was added to each well of an ELISA 96-well plate, which was incubated overnight at 4  $^{\circ}$ C and blocked with PBST solution containing 2% BSA at 37  $^{\circ}$ C for 2 h. Then, 100  $\mu$ L of the gradient-diluted IFN- $\gamma$  protein

(CLOUD-CLONE CORP, Wuhan, China) standard was added to each well and incubated at 37 °C for 2 h. Next, 50  $\mu\text{L}$  of recombinant phage at a specific copy number was added to each well and incubated at 37 °C for 1 h. After washing, 100  $\mu\text{L}$  of sterilized water was added to each well, and the mixture was heated at 95 °C for 15 min to release the binding recombinant phage DNA, which served as a template for qPCR. Five or more washes with PBST are necessary between each step to minimize nonspecific binding. Then, 10  $\mu\text{L}$  of 2  $\times$  Taq SYBR Green qPCR premix (Lablead, Beijing, China), 7  $\mu\text{L}$  of sterile water, 1  $\mu\text{L}$  of template, and 1  $\mu\text{L}$  each of 10  $\mu\text{M}$  forward (P10) and reverse primers (P11) were added to the PCR tube to a final volume of 20  $\mu\text{L}$ . A negative control was prepared using sterilized water as a template. The step program for PCR was as follows: 95 °C for 30 s, followed by 40 cycles of 95 °C for 10 s (denaturation) and 60 °C for 30 s (annealing and extension).

**2.4. Amplification Efficiency.** The recombinant phage at a concentration of  $1 \times 10^8$  copies/ $\mu\text{L}$  was serially diluted 10-fold six times to generate a series of samples with relative titers ranging from 1:10–1:10<sup>6</sup>. The phage particles were lysed by heating at 95 °C for 15 min, releasing the phage genome as a template. Then, 10  $\mu\text{L}$  of 2  $\times$  Taq SYBR Green qPCR premix (Lablead, Beijing, China), 7  $\mu\text{L}$  of sterile water, 1  $\mu\text{L}$  of template, and 1  $\mu\text{L}$  each of 10  $\mu\text{M}$  forward (P10) and reverse primers (P11) were added to the PCR tube to a final volume of 20  $\mu\text{L}$ . A negative control was prepared using sterilized water as a template. The step program for PCR was as follows: 95 °C for 30 s, followed by 40 cycles of 95 °C for 10 s (denaturation) and 60 °C for 30 s (annealing and extension). After the reaction, the logarithm of the CT values recorded in the experiment and the relative concentration of phage were analyzed to calculate the regression equation. The amplification efficiency was calculated from the slope of the regression equation as follows:

$$E(\%) = (10^{1/s} - 1) \times 100 \text{ (E: amplification efficiency, s: slope of the regression equation. )}$$

**2.5. Range and Limit of Detection.** Specifically, the PD–IMPCR assay was used to calculate the range and limit of detection by using 50  $\mu\text{L}$  of recombinant phage at a specific concentration to detect 100  $\mu\text{L}$  of each sample, which was a serially diluted protein solution. The experiment was repeated three times, and the mean of the corresponding CT value at each concentration was taken along with the logarithm of the concentration for four-parameter logistic regression analysis to obtain the equation for its curve and  $R^2$ .

The equation is  $y = (A-D)/(1+(x/C)^B)+D$ , where A, B, C, and D are parameters, x is the log concentration value, and y is the mean CT value.

The linear range (detection range) was calculated on the basis of the IC20–IC80, and the limit of detection was calculated on the basis of the IC10.

$$\text{IC10} = 0.9 \times A + 0.1 \times D$$

$$\text{IC20} = 0.8 \times A + 0.2 \times D$$

$$\text{IC80} = 0.2 \times A + 0.8 \times D$$

**2.6. Recovery Assay.** The IFN- $\gamma$  protein (CLOUD-CLONE CORP, Wuhan, China) was diluted with AIM-V medium (Gibco, CA, USA) and  $\alpha$ -MEM (Biological Industries) to generate two IFN- $\gamma$  samples with a concen-

tration of 500 pg/mL, which were detected via the PD–IMPCR assay to obtain the corresponding CT values and substituted into the standard curve equation to obtain their corresponding concentrations. The recovery was calculated according to the following equation:

$$R(\%) = (C_{\text{detected}}(\text{pg/mL})/C_0(\text{pg/mL})) \times 100\%$$

(R: recovery rate,  $C_{\text{detected}}$ : concentration of sample;  $C_0$ : concentration of sample)

**2.7. Western Blot.** Titters of each recombinant phage and wild-type M13KO7 phage (without a c-MYC tag) were detected via qPCR and diluted to  $5 \times 10^8$  copies/ $\mu\text{L}$  in PBS, and the phage genomes were released for use as samples after heating at 95 °C for 15 min. SDS–PAGE was performed at 160 V for 20 min. The protein on the gel was transferred to an NC membrane (Applygen, Beijing, China), and ten milliliters of blocking solution (TBST containing 5% skim milk) were added to the NC membrane, which was then shaken for 1 h. After blocking, the NC membrane was washed three times with TBST solution for 5 min each and then placed in an incubation chamber. Ten microliters of mouse anti-c-MYC antibody (1:1000 dilution; Lablead, Beijing, China; Cat. # M1002) were added to the incubation box, which was shaken for 5 min to mix the antibodies well, and the mixture was incubated overnight at 4 °C. The next day, the membrane was washed 5 times with TBST solution and incubated with HRP-conjugated goat antimouse antibodies (1:5000 dilution, APPLYPGEN, Beijing, China; Cat. # C2225) in a shaker at 37 °C for 1 h. The NC membrane was washed three times with TBST and immediately developed with a freshly prepared ECL (Thermo Fisher Scientific, Vacaville, CA, USA) postimaging system.

**2.8. ELISA.** Next, the IFN- $\gamma$  standard master batch (CLOUD-CLONE CORP, Wuhan, China) at 10 ng/mL was diluted to a final concentration of 250 pg/mL, and 100  $\mu\text{L}$  of the preformulated standard or sample solution was added to each well of the precoated plate. The plate was covered for 1 h at 37 °C to prevent light exposure, the liquid in the wells was discarded, 100  $\mu\text{L}$  of reaction solution A (CLOUD-CLONE CORP, Wuhan, China) was added, and the plate was covered for 1 h at 37 °C to prevent light exposure. The liquid was removed from the wells, the wells were washed three times with PBST before 100  $\mu\text{L}$  of reaction solution B (CLOUD-CLONE CORP, Wuhan, China) was added, and the wells were covered at 37 °C and kept in the dark for 0.5 h. The liquid was removed from the wells, and the wells were washed 5 times with PBST. Then, 90  $\mu\text{L}$  of substrate solution (CLOUD-CLONE CORP, Wuhan, China) was added to each well, the plates were incubated at 37 °C in the dark for 10–20 min, and 50  $\mu\text{L}$  of stop solution (CLOUD-CLONE CORP, Wuhan, China) was added to each well. The absorbance of each well was measured at 450 nm. To determine the concentration, the sample values were entered into the regression equation, and a standard curve was plotted on the basis of the standard's absorbance.

**2.9. Stability Evaluation Assay.** The newly created recombinant phage was diluted to  $1 \times 10^8$  copies/ $\mu\text{L}$  and stored for one or two months at 4 °C in a refrigerator. SYBR Green-based PD–IMPCR was performed to measure the ability of the phage to bind to IFN- $\gamma$ .

**2.10. TaqMan Probe-Based PD–IMPCR.** The TaqMan probe-based PD–IMPCR procedure is similar to the SYBR Green-based PD–IPCR procedure except for the detection steps. PD–IMPCR was performed with a TaqMan probe

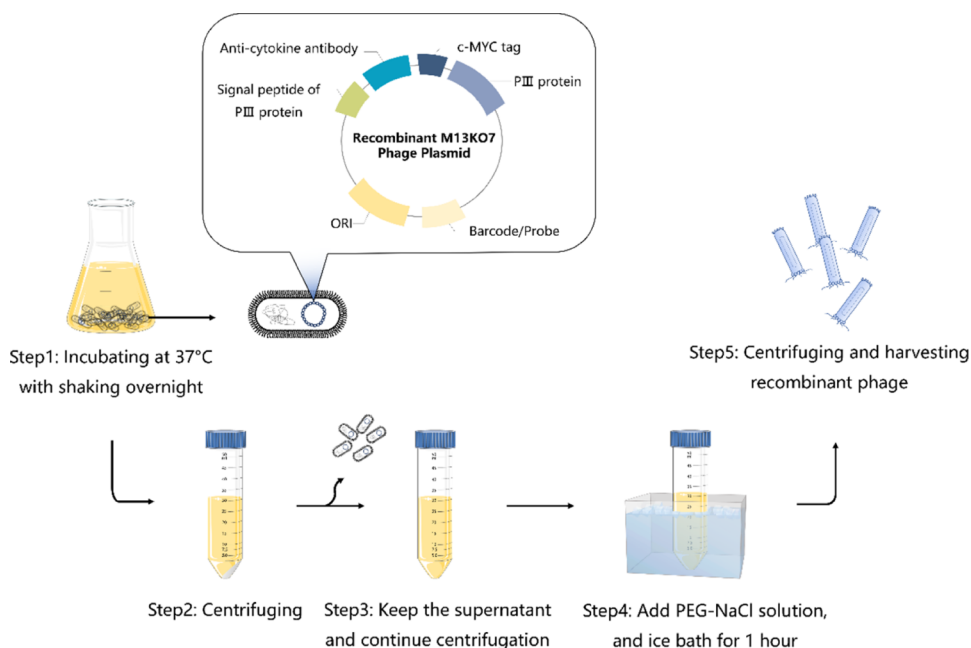


**Figure 1.** Schematic diagram of recombinant phage construction.

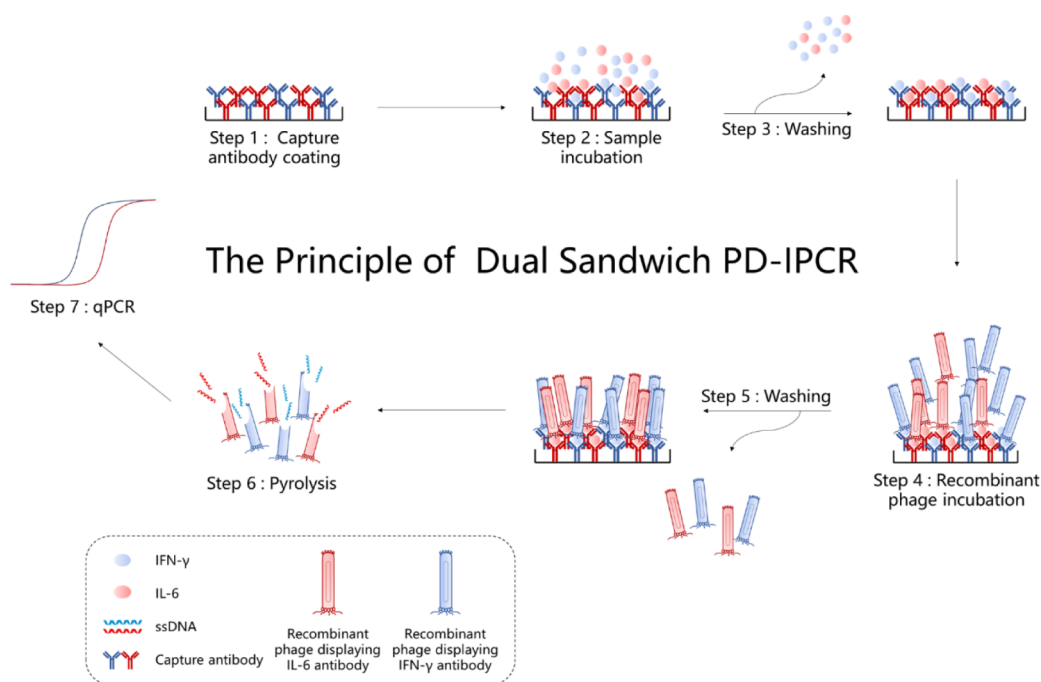


**Figure 2.** Schematic diagram of PD-IPCR.

(synthesized by Azena) via FastFire qPCR PreMix (TIAN-GEN, Beijing, China). We obtained the monoclonal antibody sequence ALD-518, which corresponds to the antibody drug clazakizumab for IL-6, in addition to the monoclonal antibody sequence IFN-HuZAF, which corresponds to the antibody drug fontolizumab for IFN- $\gamma$ , from the IMGT database. We then created an anti-IL-6 recombinant phage via the technique described in Method 2.1 and performed TaqMan probe-based PD-IPCR via the anti-IFN- $\gamma$  recombinant phage and the anti-IL-6 recombinant phage. First, 50  $\mu\text{L}$  each of anti-IL-6 and anti-IFN- $\gamma$  capture antibodies (1:250 dilution; Sino Biological, Beijing, China; Cat. # 10395-MM14) were added to each well of the ELISA 96-well plate overnight, and the plate was

blocked with 2% BSA in PBST for 2 h. One hundred microliters of gradient-diluted IL-6 and IFN- $\gamma$  protein standards (CLOUD-CLONE CORP, Wuhan, China) were added to each well, and the plate was incubated at 37  $^{\circ}\text{C}$  for 2 h. Each well was blocked with 200  $\mu\text{L}$  of M13KO7-blocking phage at a titer of  $1 \times 10^9$  copies/ $\mu\text{L}$  for 2 h. One hundred microliters of M13KO7-blocking phage at a concentration of  $5 \times 10^7$  copies/ $\mu\text{L}$  each was added. Two hundred microliters of M13KO7-blocking phage was added at a titer of  $1 \times 10^9$  copies/ $\mu\text{L}$ , and the plates were incubated at 37  $^{\circ}\text{C}$  for 2 h. Then, 100  $\mu\text{L}$  of M13KO7-ALD-518 or M13KO7-IFN-HuZAF phage mixture was added at a concentration of  $5 \times 10^7$  copies/ $\mu\text{L}$  to each well and incubated at 37  $^{\circ}\text{C}$  for 1 h.

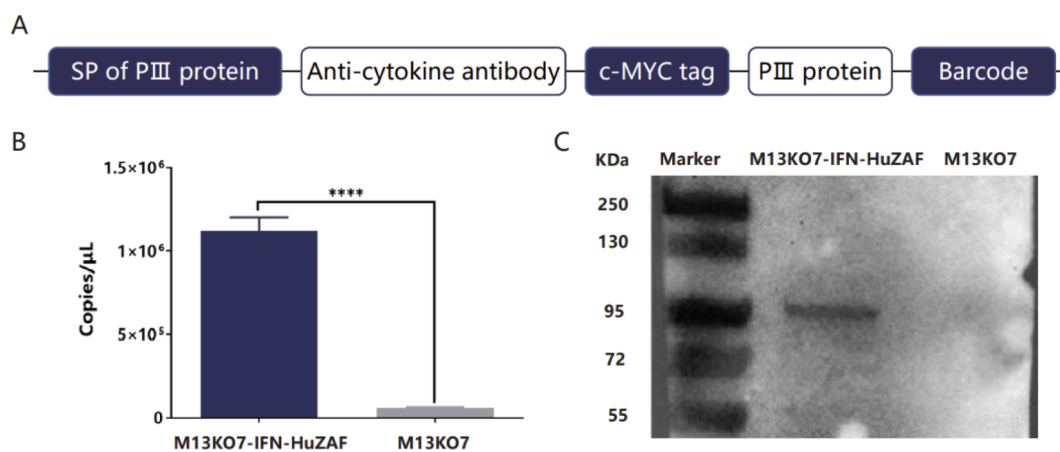


**Figure 3.** A: Construction of the recombinant phage displaying the anti-IFN- $\gamma$  antibody. Schematic diagram of the recombinant phage plasmid. B: PD-IPCR results of M13KO7-IFN-HuZAF phage binding with the c-MYC antibody. The wild-type M13KO7 phage was used as a negative control. ( $*p < 0.0001$ ,  $n = 3$ ). C: Western blot analysis of M13KO7-IFN-HuZAF phage binding to the c-MYC antibody. The wild-type M13KO7 phage was used as a negative control.

Each well was lysed by adding 100  $\mu$ L of sterile water heated at 95  $^{\circ}$ C for 20 min to release DNA from the phage as a PCR template. Five or more washes with PBST are necessary between each step to minimize nonspecific binding. TaqMan probe-based PD-IPCR was performed according to the following system: Each PCR tube consisted of 5  $\mu$ L of FastFire qPCR PreMix, 0.5  $\mu$ M of each primer (P18/P19), 0.3  $\mu$ M of each probe (P20/P21), 0.5  $\mu$ L of phage lysate as a template, and sterilized water added to a final volume of 10  $\mu$ L. The step program for PCR was 95  $^{\circ}$ C for 60 s; 40 cycles of 95  $^{\circ}$ C for 5 s (denaturation), 57  $^{\circ}$ C for 10 s (annealing), and 72  $^{\circ}$ C for 20 s (extension); and the FAM and CYS channels were selected for fluorescence signal acquisition.

**2.11. Statistical Analysis.** GraphPad Prism 8.4.2 was used to statistically evaluate the experimental results. The data were compared across groups via Student's  $t$  test, and statistical significance was indicated by  $p < 0.05$ . The experimental results are expressed as the mean  $\pm$  SEM.

### 3. RESULTS

**3.1. Principle of PD-IPCR.** The recombinant phage plasmids were constructed by inserting the antibody sequence and probe sequence into the genome of the M13KO7 phage via an In-Fusion Cloning Kit (Lablead, Beijing, China). The recombinant phage was harvested as described previously (Figure 1).

The capture antibody was used to coat the high-adsorption plate overnight at 37  $^{\circ}$ C, followed by the addition of the sample and incubation at 37  $^{\circ}$ C for 2 h. Subsequently, the incubation was terminated by washing with PBST five times, and the recombinant phage was added and incubated for 1 h at 37  $^{\circ}$ C. After incubation, the unbound recombinant phage was removed by washing with PBST, and the bound recombinant phage DNA was released by pyrolysis and detected by qPCR (Figure 2).

**3.2. Successful Construction of Recombinant Phage-Displaying Antibodies.** To verify the feasibility of PD-IPCR, we used IFN- $\gamma$  for detection. First, we constructed a recombinant M13KO7-IFN-HuZAF plasmid by inserting the anti-IFN- $\gamma$  antibody sequence and c-MYC tag in front of the PIII protein and a probe (barcode) sequence into the noncoding region of the recombinant phage, which was used

to produce a recombinant phage that can bind to IFN- $\gamma$  (Figure 3A). We subsequently performed PD-IPCR and WB experiments with anti-c-MYC antibodies to verify whether the recombinant phage successfully displayed the target protein. PD-IPCR revealed that the M13KO7-IFN-HuZAF phage specifically bound to the anti-c-MYC antibody, unlike the wild-type M13KO7 phage (Figure 3B,  $n = 3$ ,  $p < 0.0001$ ). Western blot assays demonstrated that the M13KO7-IFN-HuZAF phage contained the target protein, whereas the wild-type M13KO7 phage, which served as a negative control, did not express the fusion protein (Figure 3C). The above results indicate that we successfully constructed a recombinant phage that displayed fusion proteins.

**3.3. PD-IPCR Exhibits Superior Specificity.** The specificity of PD-IPCR was verified by the ability of the recombinant M13KO7-IFN-HuZAF phage displaying anti-IFN- $\gamma$  antibodies to bind the IFN- $\gamma$ , TNF- $\alpha$ , and IL-6 proteins, while water was used as a negative control. The results demonstrated that the M13KO7-IFN-HuZAF phage with the anti-IFN- $\gamma$  antibody specifically bound to the IFN- $\gamma$  protein but not the IL-6 or TNF- $\alpha$  proteins. The binding copy number for IL-6 and TNF- $\alpha$  was comparable to that of the negative control, underscoring the targeted binding capability and high specificity of our PD-IPCR method (Figure 4A).

**3.4. Using the Recombinant Phage Genome as a qPCR Template.** Amplification efficiency experiments were performed via the use of phage genomes as qPCR templates, which were obtained via gradient dilution and pyrolysis of the recombinant phage, and the results are shown in Figure 4B. The linear correlation of the obtained regression equation was good, with  $R^2 = 0.9967$ , and the amplification efficiency  $E = 90.1\%$  was within the ideal range of 90–110%. Therefore, it is feasible to use the recombinant phage genome obtained after thermal lysis as the template for qPCR via this method.

**3.5. Scope and Limitations of PD-IPCR for Detecting IFN- $\gamma$ .** We used the M13KO7-IFN-HuZAF phage at  $1 \times 10^8$  copies/ $\mu$ L. PD-IPCR was used to detect 7.81 pg/mL to 1 ng/mL IFN- $\gamma$  protein, and the experiment was repeated three times. The mean CT values of the three replicate experiments were used to calculate the linear regression equation, and the equation was  $y = -6.296x + 29.76$ ,  $R^2 = 0.9921$  (Figure 4C). The detection range of this method is 31.25–500 pg/mL, and the

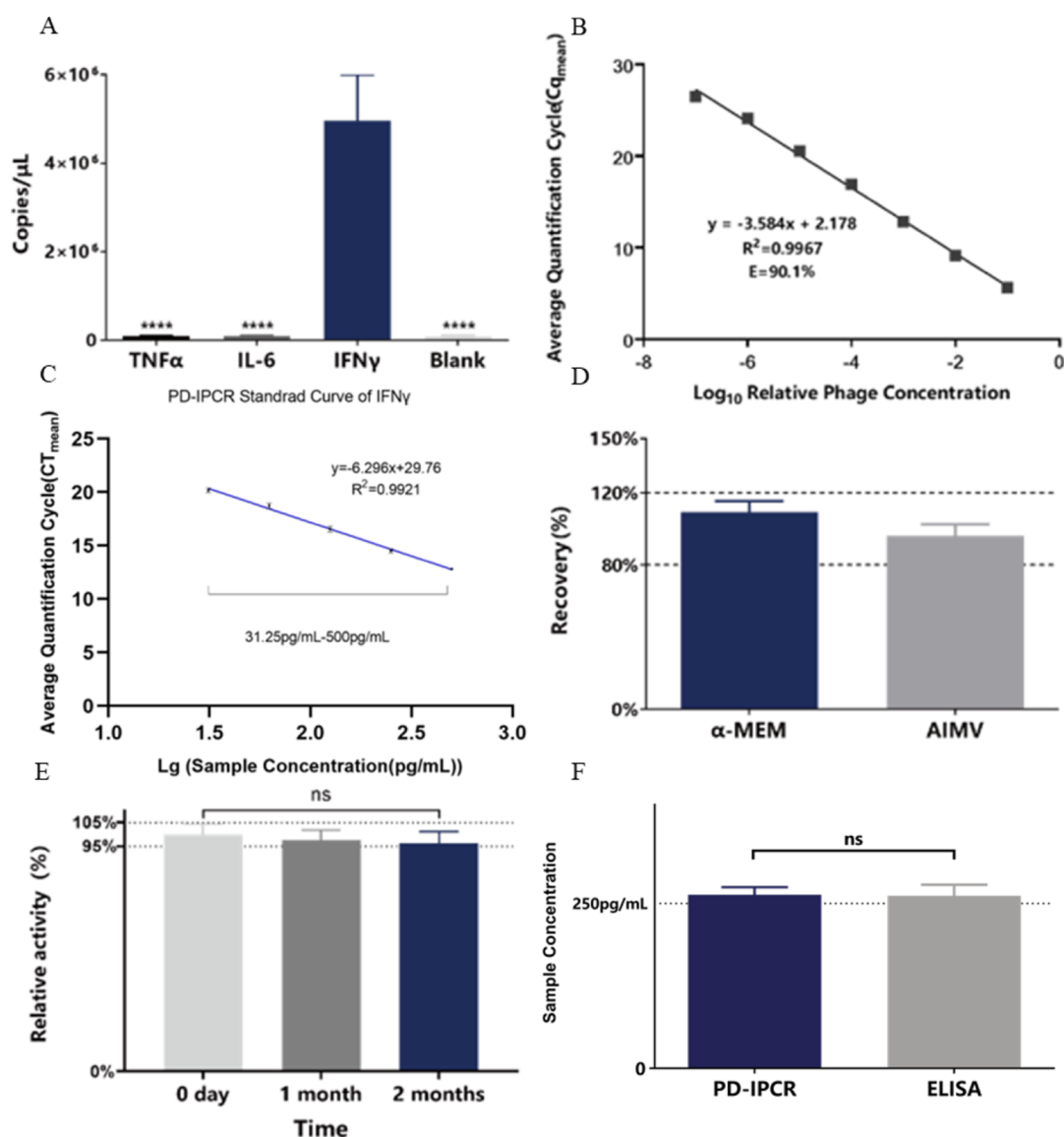


**Figure 4.** A: Specificity of PD-IMPCR. B: Standard curve of qPCR amplification efficiency obtained with 10-fold serial dilutions of the recombinant phage, plotted with the quantification cycle ( $C_q$ ) and the  $\text{log}_{10}$  phage concentration. The regression parameters are shown on the left. C: Standard curve of PD-IMPCR for detecting IFN- $\gamma$ . D: Results of the recovery assay. E: Stability of the recombinant phage. F: ELISA results compared with the PD-IMPCR results.

limit of detection is 26.30 pg/mL based on the blank control group.

**3.6. Culture Medium Does Not Affect PD-IMPCR Detection.** To validate whether the cell culture medium affects the results of the PD-IMPCR assay,  $\alpha$ -MEM and AIM-V were used to dilute the IFN- $\gamma$  protein for recovery assays. As shown in Figure 4D, the recovery rate of  $\alpha$ -MEM was  $109.23 \pm 6.03\%$  ( $n = 3$ ), whereas the recovery rate of AIM-V medium was  $96.05 \pm 6.50\%$  ( $n = 3$ ), both of which are in accordance with the ideal recovery range of 80–120%.

**3.7. Validation of the Stability of the Recombinant Phage.** To confirm the stability of the recombinant phage, we stored it at 4  $^{\circ}\text{C}$  for one and two months. We subsequently measured the impact of this storage temperature on IFN- $\gamma$  by comparing the quantification results obtained with freshly created recombinant phage to those of the standard. The findings demonstrated that (Figure 4E) the prepared recombinant phage retained strong stability and good

detection ability after storage at 4  $^{\circ}\text{C}$  for a minimum of two months. Compared with freshly prepared recombinant phages,  $99 \pm 1.16\%$  and  $98 \pm 2.65\%$  of the recombinant phages were retained after storage for one month and two months, respectively.

**3.8. PD-IMPCR Compared with ELISA.** To further validate the accuracy and precision of PD-IMPCR, we compared PD-IMPCR with ELISA by analyzing the same sample, which contained 250 pg/mL IFN- $\gamma$  protein. We substituted the  $CT$  values from PD-IMPCR and the  $OD$  values from ELISA into their respective standard curve equations to calculate the concentrations detected by each method. These two concentrations were further compared to verify the accuracy of the PD-IMPCR assay. Our findings indicated that the PD-IMPCR results were consistent with the ELISA results, with no significant differences (Figure 4F). Consequently, it is feasible to use PD-IMPCR to detect cytokines.

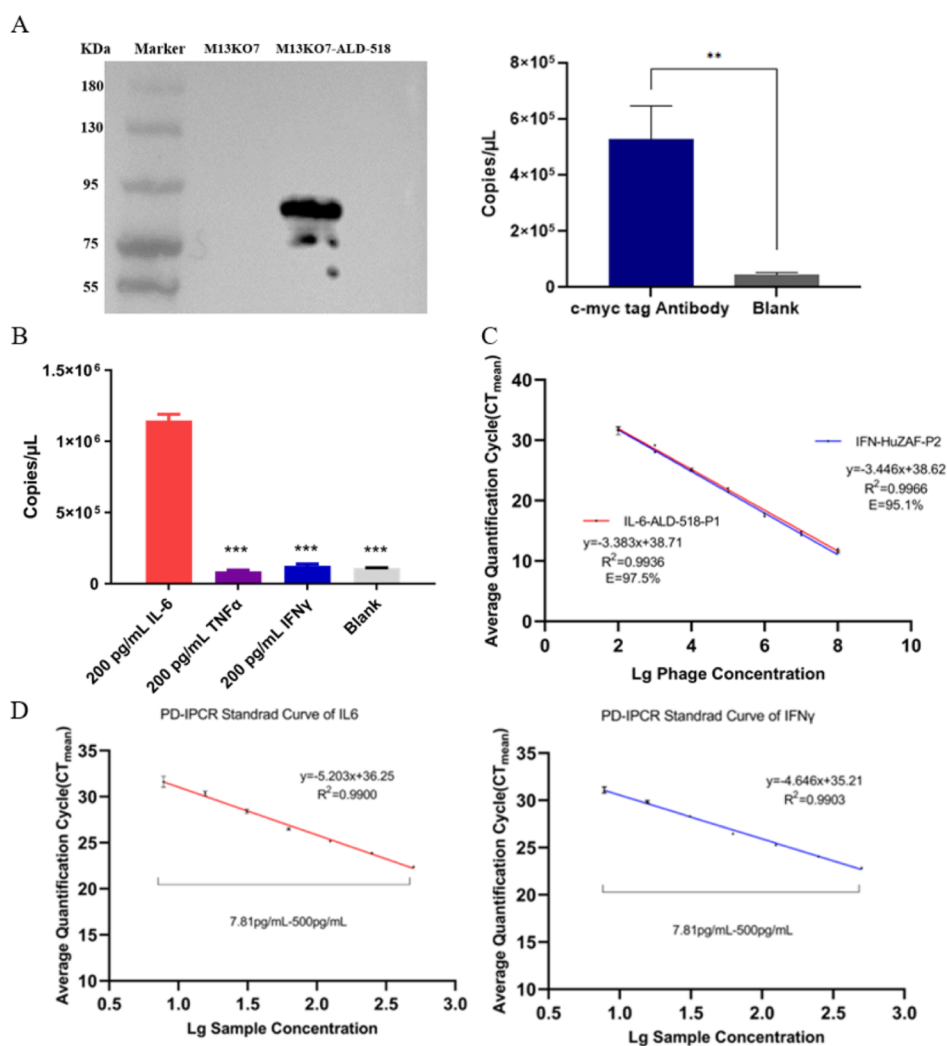


**Figure 5.** A. The results of the recombinant phage and the IL-6 antibody binding with the c-MYC tag antibody ( $n = 3$ ) (\*\* $p < 0.01$ , \*\*\* $p < 0.001$ ). B. The results of the validation experiments demonstrating the antigen-binding activity of the recombinant phage with the IL-6 antibody (\*\* $p < 0.001$ ). C. Validation of the multiplex qPCR amplification efficiency via the recombinant phage probe method ( $n = 3$ ). D. Standard curve graphs of the dual assay method, which is based on a double-antibody sandwich and PD-IPCR ( $n = 3$ ).

**3.9. Quantitative PD-IPCR Assay.** We created an anti-IL-6 M13KO7-ALD-518 recombinant phage via the anti-IFN- $\gamma$  recombinant phage design method. We subjected the recombinant phage to Western blot analysis with a c-myc antibody following high-temperature denaturation to verify the ability of the c-myc tag to recognize the antibody in vitro. After the recombinant phage was added and washed to eliminate nonspecific binding, the phage in the wells was detected by qPCR and contrasted with blank wells that were not coated with the antibody to eliminate nonspecific phage binding. Western blot and qPCR analyses confirmed the expression of the M13KO7-ALD-518 anti-IL-6 fusion protein and its ability to bind IL-6. (Figure 5A). The PD-IPCR results revealed that the recombinant M13KO7-ALD-518 phage had specific anti-IL-6 effects on IFN- $\gamma$ , TNF- $\alpha$  and IL-6 (Figure 5B). In the same reaction system, we used the TaqMan probe-based PD-IPCR assay to simultaneously detect IFN- $\gamma$  and IL-6. First, to distinguish between the M13KO7-IFN-HuZAF and M13KO7-ALD-518 recombinant phages, distinct probe binding sequences were introduced into each of the two recombinant phages to create the M13KO7-IFN-HuZAF probe and the M13KO7-ALD-518 probe. We designed a

blank phage, M13KO7, for blocking to prevent the qPCR primers from recognizing nonspecific sequences, enhancing the assay's specificity under detection conditions. The results of this assay confirmed that the amplification efficiency of the anti-IFN- $\gamma$  recombinant phage in the same reaction system was 97.5%, whereas that of the anti-IL-6 recombinant phage in the same reaction system was 95.1%. (Figure 5C). This system's detection range for IL-6 and IFN- $\gamma$  was 7.81 pg/mL to 500 pg/mL. The results of Method 2.5 showed that distinct target molecules can be qualitatively and quantitatively detected in the same assay. Compared with that of the blank control group, the limit of detection for IL-6 was 6.46 pg/mL, and for IFN- $\gamma$ , it was 6.13 pg/mL (Figure 5D). This result demonstrated that the method can qualitatively and quantitatively detect different target molecules in the same assay.

#### 4. DISCUSSION

Cytokines, crucial components of the immune system, play a significant role in disease development. Therefore, the ability to detect cytokines quantitatively is important in clinical diagnostics and drug development. The network and

pleiotropic nature of cytokines necessitate the development of multiplex cytokine assays.<sup>11,23</sup> ELISAs are widely used for cytokine detection but lack multiplexing capabilities. In contrast, commonly used multiplex assays, such as CBA, Luminex, and MSD, have a broader detection range but are disadvantaged by costly kits and the need for specialized or sophisticated detection instruments. Therefore, developing a high-throughput and inexpensive cytokine assay is important. As a class of natural protein–nucleic acid coupled carriers, phages have great potential for detection and analysis; therefore, we wanted to investigate the feasibility of the simultaneous qualitative and quantitative detection of different cytokines within the same system and designed phages with different probes that can carry different cytokine scFvs for the detection of samples. On the basis of the results of this study, it was preliminarily verified that short DNA sequences, such as probes and barcodes, can be used to measure the class and number of phages by inserting them into the genome of M13 phages with good linear correlation, which provides an idea for the application of phages in high-throughput detection.

We established the PD–IMPCR method, which combines phage display and immune PCR advantages for the quantification of IFN- $\gamma$  and IL-6. In phage monovalent display systems, recombinant phages often have many wild-type fragments in the PIII protein, which may interfere with the binding of the antibody and the target, increasing the nonspecific binding of the detection system. We opted for a phage multivalent display system over the common monovalent system in PD–IPCR, enhancing the binding efficiency of the antibody fragment to the target protein. Recombinant phages that can specifically bind cytokines were constructed by inserting a nanobody sequence (the produced scFv was not thoroughly examined; however, further research is needed for improved specific binding activity to improve PD–IMPCR detection) in front of the pIII protein of wild-type M13KO7. We confirmed that DNA from thermally lysed recombinant phages serves effectively as a qPCR template. The efficiency of our experiment was 90.1%, which corresponded with the ideal range of 90–110% for qPCR amplification reactions. Therefore, we conducted a series of experiments to validate the feasibility of using recombinant phages displaying anticytokine antibodies to detect cytokines, such as IFN- $\gamma$ . The detection range of IFN- $\gamma$  recombinant protein utilizing PD–IMPCR was 31.25 pg/mL–500 pg/mL, with a detection limit of 26.30 pg/mL; this result was similar to that of commercially available ELISA kits, but the detection limit was slightly greater. The purpose of sandwich assays is to sandwich a cytokine between two specific antibodies that bind to the cytokine with two noncompeting epitopes of that cytokine.<sup>10</sup> Obtaining sequences of commercially available capture and detection antibody pairs is difficult; thus, the cytokine binding sites of the detection antibodies displayed by the recombinant phage used in this study may conflict with those of the capture antibodies, which may account for the narrow scope of this assay. Specificity experiments demonstrated that our recombinant phage displayed antibodies that specifically bind to target proteins, highlighting the superior specificity and multicytokine detection potential of PD–IMPCR. The recoveries were 96.05% for AIM-V medium and 109% for  $\alpha$ -MEM, indicating that the PD–IMPCR assay developed for the quantification of cytokines in actual complete medium samples has good precision and great reproducibility; these results also indicated that the complex matrix did not interfere with the assay.

Stability tests revealed that short-term storage at 37 °C did not diminish the activity of our recombinant phage. Therefore, the activity of the recombinant phage is not easily altered by temperature changes during transport. In addition, low-temperature storage theoretically helps maintain the activity of the recombinant phage, which indicates that PD–IMPCR shows great potential for commercialization. For multiplex cytokine detection, we integrated a probe (barcode) sequence into the noncoding region of the recombinant phage and employed TaqMan probe qPCR, enabling simultaneous detection of multiple signals in one reaction. Compared with the SYBR Green dye-based system, this probe method has greater specificity and sensitivity. The system also produces fluorescent signals only after the luminescent moiety at the 5' end of the probe primer binds to the target site and is completely excised, which potentially increases the assay specificity and detection range of PD–IMPCR. The results showed that the amplification efficiency, linearity, and detection sensitivity of the dual PD–IPCR assay constructed in the present study were superior to those of the single-cytokine PD–IPCR assay based on the SYBR Green method. This improvement was achieved by designing an M13KO7-blocking recombinant phage that cannot be recognized by qPCR primers to further reduce nonspecific interference from the reaction background. These findings provide opportunities for developing multiple detection methods using phage immunoprecipitation and multivalent antibody display systems. Owing to the incredibly low cost of preparing phages, there are broad application prospects for multiple PD–IPCR detection methods. In the future, the probe sequences in the phage genome can be substituted with the barcode sequences needed for DNA sequencing, which can be combined with high-throughput sequencing technology to greatly improve the throughput of protein detection.

## 5. CONCLUSIONS

In conclusion, a linear range and detection limit were established; a dual antibody display system was successfully demonstrated against IL-6 and IFN- $\gamma$  on the basis of the M13KO7 phage; and the viability of quantitatively detecting multiple protein targets was demonstrated via phage DNA analysis. This method is stable because of its physicochemical properties and low preparation complexity, heralding a promising future for its broader application.

## ■ ASSOCIATED CONTENT

### Data Availability Statement

All relevant data are within the manuscript and its additional files.

### Supporting Information

The Supporting Information is available free of charge at <https://pubs.acs.org/doi/10.1021/acsomega.4c09624>.

Initial plasmid sequences (Table S1); Raw image of Western blot (Figure S1 and Figure S2) (PDF)

## ■ AUTHOR INFORMATION

### Corresponding Author

Jianxun Wang – School of Life Sciences, Beijing University of Chinese Medicine, Beijing 102488, China;  
Email: [jianxun.wang@bucm.edu.cn](mailto:jianxun.wang@bucm.edu.cn)



## Authors

**Zhou Hu** – School of Life Sciences, Beijing University of Chinese Medicine, Beijing 102488, China; [orcid.org/0009-0000-0381-3849](https://orcid.org/0009-0000-0381-3849)

**Shen Li** – School of Life Sciences, Beijing University of Chinese Medicine, Beijing 102488, China

**Hanyi Chen** – School of Life Sciences, Beijing University of Chinese Medicine, Beijing 102488, China

**Zhuoying Yu** – School of Life Sciences, Beijing University of Chinese Medicine, Beijing 102488, China

**Wenjuan Wang** – School of Life Sciences, Beijing University of Chinese Medicine, Beijing 102488, China

**Xiaotian Zhang** – School of Life Sciences, Beijing University of Chinese Medicine, Beijing 102488, China

**Mengyuan Yu** – School of Life Sciences, Beijing University of Chinese Medicine, Beijing 102488, China

Complete contact information is available at:

<https://pubs.acs.org/10.1021/acsomega.4c09624>

## Author Contributions

<sup>#</sup>S.L. and H.C. contributed equally: Z.H., S.L., H.C.; J.W. and H.C. conceived and designed this study; Z.H. and S.L. wrote the manuscript; H.C., Z.H. and S.L. performed the majority of the experiments; and Z.Y., W.W., X.Z. and M.Y. assisted in the experiments. All the authors read and approved the final version of the manuscript.

## Funding

This study was supported by the Research Start-up Funding Program for High-level Talents of Beijing University of Chinese Medicine (9011451310032).

## Notes

The authors declare no competing financial interest.

## REFERENCES

- (1) Borish, L. C.; Steinke, J. W. 2. Cytokines and chemokines. *J. Allergy Clin. Immunol.* **2003**, *111* (2), S460–S475.
- (2) Kelso, A. Cytokines: Principles and prospects. *Immunol. Cell Biol.* **1998**, *76* (4), 300–317.
- (3) Leonard, W. J. The defective gene in X-linked severe combined immunodeficiency encodes a shared interleukin receptor subunit: Implications for cytokine pleiotropy and redundancy. *Curr. Opin. Immunol.* **1994**, *6* (4), 631–635.
- (4) Ozaki, K.; Leonard, W. J. Cytokine and Cytokine Receptor Pleiotropy and Redundancy\*. *J. Biol. Chem.* **2002**, *277* (33), 29355–29358.
- (5) Fajgenbaum, D. C.; June, C. H. Cytokine Storm. *N. Engl. J. Med.* **2020**, *383* (23), 2255–2273.
- (6) Tisoncik, J. R.; Korth, M. J.; Simmons, C. P.; Farrar, J.; Martin, T. R.; Katze, M. G. Into the Eye of the Cytokine Storm. *Microbiol. Mol. Biol. Rev.* **2012**, *76* (1), 16–32.
- (7) Liu, C.; Chu, D.; Kalantar-Zadeh, K.; George, J.; Young, H. A.; Liu, G. Cytokines: From Clinical Significance to Quantification. *Adv. Sci.* **2021**, *8* (15), 2004433.
- (8) Gay, F.; Romeo, B.; Martelli, C.; Benyamina, A.; Hamdani, N. Cytokines changes associated with electroconvulsive therapy in patients with treatment-resistant depression: a Meta-analysis. *Psychiatry Res.* **2021**, *297*, 113735.
- (9) Nikles, S.; Monschein, M.; Zou, H. Metabolic profiling of the traditional Chinese medicine formulation Yu Ping Feng San for the identification of constituents relevant for effects on expression of TNF- $\alpha$ , IFN- $\gamma$ , IL-1 $\beta$  and IL-4 in U937 cells. *J. Pharm. Biomed. Anal.* **2017**, *145*, 219–229.
- (10) de Jager, W.; Rijkers, G. T. Solid-phase and bead-based cytokine immunoassay: A comparison. *Methods* **2006**, *38* (4), 294–303.
- (11) Keustermans, G. C. E.; Hoeks, S. B. E.; Meering, J. M.; Prakken, B. J.; de Jager, W. Cytokine assays An assessment of the preparation and treatment of blood and tissue samples. *Methods* **2013**, *61* (1), 10–17.
- (12) Morgan, E.; Varro, R.; Sepulveda, H.; et al. Cytometric bead array: a multiplexed assay platform with applications in various areas of biology. *Clin. Immunol.* **2004**, *110* (3), 252–266.
- (13) Dunbar, S. A.; Vander Zee, C. A.; Oliver, K. G.; Karem, K. L.; Jacobson, J. W. Quantitative, multiplexed detection of bacterial pathogens: DNA and protein applications of the Luminex LabMAP™ system. *J. Microbiol. Methods* **2003**, *53* (2), 245–252.
- (14) Dabitao, D.; Margolick, J. B.; Lopez, J.; Bream, J. H. Multiplex measurement of proinflammatory cytokines in human serum: comparison of the Meso Scale Discovery electrochemiluminescence assay and the Cytometric Bead Array. *J. Immunol. Methods* **2011**, *372* (1–2), 71–77.
- (15) Guo, Y. C.; Zhou, Y. F.; Zhang, X. E.; et al. Phage display mediated immuno-PCR. *Nucleic Acids Res.* **2006**, *34* (8), No. e62.
- (16) Tan, Y.; Tian, T.; Liu, W.; Zhu, Z.; Yang, C. Y. Advance in phage display technology for bioanalysis. *Biotechnol. J.* **2016**, *11* (6), 732–745.
- (17) Sano, T.; Smith, C. L.; Cantor, C. R. Immuno-PCR: Very Sensitive Antigen Detection by Means of Specific Antibody-DNA Conjugates. *Science* **1992**, *258* (5079), 120–122.
- (18) Wang, X.; He, Q.; Xu, Y.; et al. Anti-idiotypic VHH phage display-mediated immuno-PCR for ultrasensitive determination of mycotoxin zearalenone in cereals. *Talanta* **2016**, *147*, 410–415.
- (19) Monjezi, R.; Tan, S. W.; Tey, B. T.; Sieo, C. C.; Tan, W. S. Detection of hepatitis B virus core antigen by phage display mediated TaqMan real-time immuno-PCR. *J. Virol. Methods* **2013**, *187* (1), 121–126.
- (20) Ren, X.; Zhang, Q.; Wu, W.; et al. Anti-idiotypic nanobody-phage display-mediated real-time immuno-PCR for sensitive, simultaneous, and quantitative detection of total aflatoxins and zearalenone in grains. *Food Chem.* **2019**, *297*, 124912.
- (21) Liu, X.; Xu, Y.; Xiong, Y.-H.; Tu, Z.; Li, Y.-P.; He, Z.-Y.; Qiu, Y.-L.; Fu, J.-H.; Gee, S. J.; Hammock, B. D. VHH Phage-Based Competitive Real-Time Immuno-Polymerase Chain Reaction for Ultrasensitive Detection of Ochratoxin A in Cereal. *Anal. Chem.* **2014**, *86* (15), 7471–7477.
- (22) Rezaei, Z. S.; Shahangian, S. S.; Hasannia, S.; Sajedi, R. H. Development of a phage display-mediated immunoassay for the detection of vascular endothelial growth factor. *Anal. Bioanal. Chem.* **2020**, *412* (27), 7639–7648.
- (23) Chauhan, P.; Nair, A.; Patidar, A.; Dandapat, J.; Sarkar, A.; Saha, B. A primer on cytokines. *Cytokine* **2021**, *145*, 155458.